Analytical study of Al₂O₃-Cu/water micropolar hybrid nanofluid in a porous channel with expanding/contracting walls in the presence of magnetic field

M. Mollamahdi, M. Abbaszadeh*, and Gh.A. Sheikhzadeh

Department of Mechanical Engineering, University of Kashan, Kashan, Iran.

Abstract. Forced convection fluid flow and heat transfer were investigated in a porous channel with expanding or contracting walls, which was filled with Al₂O₃-Cu/water micropolar hybrid nanofluid in the presence of magnetic field. In order to solve the governing equations analytically, the least square method was employed. The hot bottom wall was cooled by the coolant fluid, which was injected into the channel from the top wall. The range of nanoparticles volume fraction (90% Al₂O₃ and 10% Cu by volume) was between 0% and 2%. The effects of consequential parameters such as Reynolds number, Hartmann number, micro rotation factor, and nanoparticles volume fraction on velocity and temperature profiles were examined. The results show that with increasing Reynolds number, the values of temperature and micro rotation profiles decrease. Furthermore, when the hybrid nanofluid is used, compared to common nanofluid, the heat transfer coefficient will increase significantly. It is also observed that when the Hartmann number increases, Nusselt number increases, too.

1. Introduction

As long as obtaining the solution to nonlinear differential equations is difficult, the weighted residual methods emerge as new powerful and straightforward approaches to solve these kinds of equations. The most famous weighted residual method, which has commonly been used in recent years, is Least Square Method (LSM). In recent years, numerous problems have been solved by the least square method. Aziz and Bouaziz [1]

employed the least square method to prognosticate the performance of the longitudinal fins. They found that the least square method was simpler than other analytical methods. Hatami and Ganji [2] used the least square method to investigate heat transfer in a microchannel heat sink, which was cooled by Cu-water nanofluid. They also studied natural convection of a non-Newtonian nanofluid flow between two vertical flat plates through this method [3]. Electrohydrodynamic flow in a circular cylindrical conduit was examined by Ghasemi et al. [4]. They demonstrated that results of the least square method coincided with the numerical results, but the least square method was more acceptable and simpler, and needed fewer computations than homotopy analysis method did. Hatami et al. [5] analytically studied magneto-hydrodynamic

---

*. *Corresponding author.*
E-mail address: abbaszadeh.mahmoud@gmail.com (M. Abbaszadeh)

Jeffery-Hamel nanofluid flow in non-parallel walls using Differential Transformation Method (DTM) and least square method. They showed that the least square method was more accurate than differential transformation method. In other analytical investigations, Fakour et al. [6,7] employed the least square method to study flow field and heat transfer in a porous channel in the presence of a transverse magnetic field. The effect of thermal radiation on flow field and heat transfer in a thin liquid film in a porous medium was investigated by Darzi et al. [8] using the least square method.

Enhancement of heat transfer in industrial and engineering applications is a consequential issue which many researchers have dealt with over the past few years. Although many methods, such as using pure nanofluids [9-12], have been introduced to enhance heat transfer in such applications, using the hybrid nanofluid is an innovative means which has received striking consideration in the last decade. As early as 1999, Wang et al. [13] measured effective thermal conductivity of mixtures of fluids and nanoparticles. They used water as a base fluid and CuO and Al_2O_3 nanoparticles. They demonstrated that the thermal conductivity of nanoparticle-fluid mixture was higher than that of nanofluid. Selvakumar and Suresh [14] experimentally investigated the effect of using Al_2O_3-Cu/water hybrid nanofluid in cooling of electronic components. They observed that the convective heat transfer coefficient of the heat sink significantly increased when hybrid nanofluid was used as the working fluid instead of water. In another experimental investigation, Madhesh et al. [15] studied the heat transfer potential of Cu-TiO_2 hybrid nanofluids in a tube-type counter-flow heat exchanger. The experimental correlation for Cu-TiO_2 hybrid nanofluid which they found anticipated the experimental data with maximum deviations of +7% and −4% in all volume concentrations. They also demonstrated that the convective heat transfer coefficient increased by 52% when hybrid nanofluids were used. Esfe et al. [16] found an experimental correlation for Ag-MgO/water hybrid nanofluid with the particle diameters of 40(MgO) and 25(Ag) nm and nanoparticle volume fraction range between 0% and 2%. Other researches dedicated to the use of hybrid nanofluid in heat transfer are presented in [17-24].

In order to get a better insight into the behavior of fluid flow, it is necessary to consider the effect of rotating micro-constituents on fluid and that is where the use of micropolar theory comes to the scene. In 1966, the theory of micropolar fluids was introduced by Eringen [25]. Nadeem et al. [26] studied axisymmetric stagnation flow of a micropolar nanofluid in a moving cylinder with finite radius. They investigated the effect of micro rotation parameter on the velocity and temperature profiles, and found that when the microp-

olar parameter increased, the velocity and temperature profiles showed increasing behavior. Flow field and heat transfer of an incompressible micropolar fluid in a channel with expanding or contracting walls was investigated by Si et al. [27]. They demonstrated that the microrotation velocity was zero at the center of the channel due to the opposite directions of the microrotation velocity. They also observed that for a specified boundary condition, the values of the microrotation velocity were not zero at the walls. Bourantas and Loukopoulos [28] theoretically studied differentially heated natural convection of micropolar nanofluid of Al_2O_3-water in a cavity. They observed that the micro rotation of nanoparticles in suspension decreased the overall heat transfer. Sheikholeslami et al. [29] conducted an analytical solution to investigate micropolar fluid flow in a channel subject to a chemical reaction. According to their results, the velocity and micro rotation profiles decreased as Reynolds number increased. Very recently, Cao et al. [30] studied the flow of a micropolar fluid through a porous channel with deforming walls. They examined the effect of expansion ratio on micro rotation profiles and found out that the micro rotation change was concavity at the center of the channel.

In view of the above-mentioned literature, it can be found that the flow field and heat transfer of micropolar hybrid nanofluid in a porous channel have not received attention and examination of them still remains to be addressed. Therefore, in the present study, the flow field and heat transfer of Al_2O_3-Cu/water micropolar hybrid nanofluid are investigated in a channel with porous wall in the presence of magnetic field. The effects of various parameters such as Reynolds number, Hartmann number, and expanding ratio on velocity, temperature, and micro rotation profiles are studied. Moreover, the analytical results are compared with fourth-order Runge-Kutta-Fellberg numerical method and a good conformity is achieved.
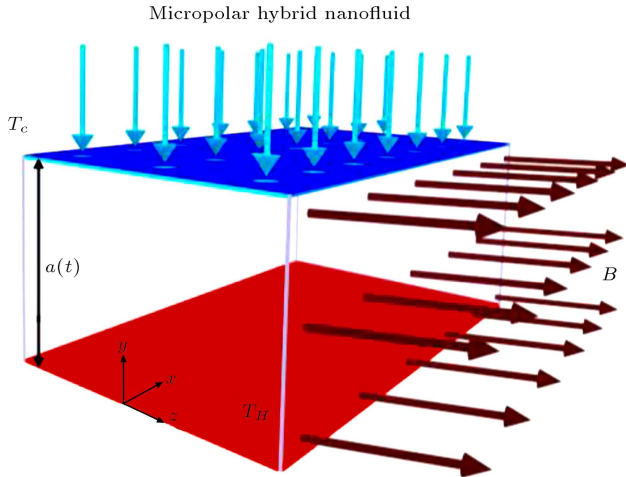
2. Problem formulation

A two-dimensional laminar flow of Al_2O_3-Cu/water micropolar hybrid nanofluid is studied in porous channel using the least square method. The geometry of the problem is depicted in Figure 1. The bottom wall is hot and is cooled by the micropolar hybrid nanofluid, which is injected into the channel from the porous top wall. The distance between the two walls is $a(t)$ and the x-axis coincides with the bottom wall. The bottom and top walls of the channel are maintained at temperatures of T_2 and T_1, respectively. Thermo-physical properties of water as a base fluid and Al_2O_3 and Cu nanoparticles are presented in Table 1.

The range of nanoparticles volume fraction (90%

	ρ (kg/m^3)	c_p (j/kg K)	K (W/mK)	σ (Ω.m)$^{-1}$	Pr
Al$_2$O$_3$	3970	765	25	1×10^{-10}	—
Cu	3954	383	400	5.96×10^7	—
Pure water	997.1	4179	0.613	0.05	6.2

Figure 1. Schematic of the problem.

Al$_2$O$_3$ and 10% Cu by volume) is between 0% and 2%. The hybrid nanofluid density [31,32], heat capacity [32,33] electrical conductivity [34,35], viscosity, and thermal conductivity [18] are obtained from the following relations, respectively:

$$\rho_{nf} = (1 - \phi)\rho_f + \phi\rho_s, \tag{1}$$

$$\rho_{nf}c_{p_{nf}} = (1 - \phi)c_{p_f}\rho_f + \phi c_{p_s}\rho_s, \tag{2}$$

$$\frac{\sigma_{nf}}{\sigma_f} = 1 + \frac{3\left(\frac{\sigma_p}{\sigma_f} - 1\right)\phi}{\left(\frac{\sigma_p}{\sigma_f} + 2\right) - \left(\frac{\sigma_p}{\sigma_f} - 1\right)\phi}, \tag{3}$$

$$\frac{\mu_{nf}}{\mu_f} = -1283\phi^2 + 8431\phi + 0.9454, \tag{4}$$

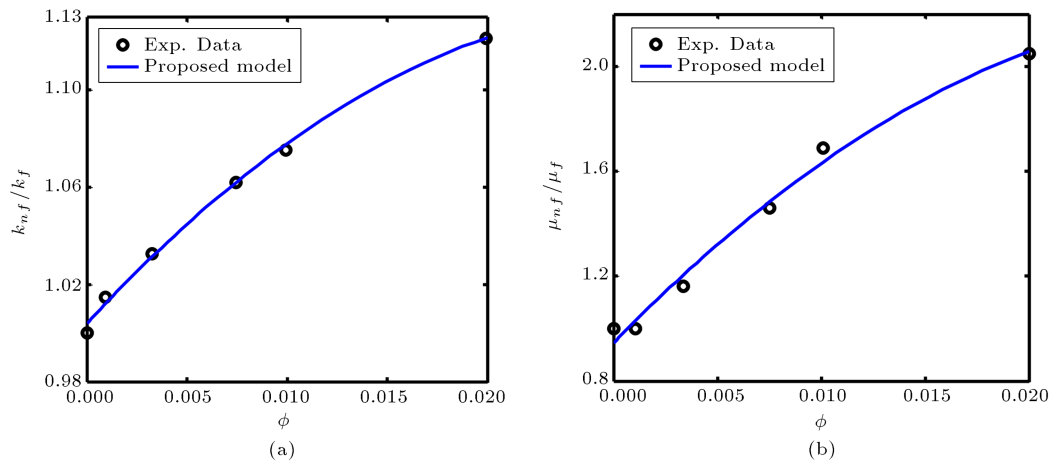$$\frac{k_{nf}}{k_f} = -151.5\phi^2 + 8.916\phi + 1.004. \tag{5}$$

It is noteworthy to say that Relations (4) and (5) are derived from an experimental model [18]. In order to correlate these relations, two graphs are fitted to the experimental data, which is illustrated in Figure 2.

The governing equations of the problem are given by [36,37]:

$$\frac{\partial u}{\partial x} + \frac{\partial v}{\partial y} = 0, \tag{6}$$

$$\rho_{nf}\left(\frac{\partial u}{\partial t} + u\frac{\partial u}{\partial x} + v\frac{\partial u}{\partial y}\right) = -\frac{\partial P}{\partial x}$$
$$+ (\mu_{nf} + \kappa)\left[\frac{\partial^2 u}{\partial x^2} + \frac{\partial^2 u}{\partial y^2}\right] + \kappa\frac{\partial N}{\partial y} - \sigma_{nf}B^2 u, \tag{7}$$

$$\rho_{nf}\left(\frac{\partial v}{\partial t} + u\frac{\partial v}{\partial x} + v\frac{\partial v}{\partial y}\right) = -\frac{\partial P}{\partial y}$$
$$+ (\mu_{nf} + \kappa)\left[\frac{\partial^2 v}{\partial x^2} + \frac{\partial^2 v}{\partial y^2}\right] - \kappa\frac{\partial N}{\partial x}, \tag{8}$$

Figure 2. Fitting graphs to the experimental data.

$$\rho_{nf}\left(\frac{\partial N}{\partial t}+u\frac{\partial N}{\partial x}+v\frac{\partial N}{\partial y}\right)=-\frac{\kappa}{j}\left(2N+\frac{\partial u}{\partial y}-\frac{\partial v}{\partial x}\right)$$

$$+\left(\mu_{nf}+\frac{\kappa}{2}\right)\left[\frac{\partial^2 N}{\partial x^2}+\frac{\partial^2 N}{\partial y^2}\right], \qquad (9)$$

$$\rho_{nf}\left(\frac{\partial T}{\partial t}+u\frac{\partial T}{\partial x}+v\frac{\partial T}{\partial y}\right)=\frac{k_{nf}}{c_{p_{nf}}}\frac{\partial^2 T}{\partial y^2}, \qquad (10)$$

where u and v are the velocity components in the x and y directions, respectively. σ is electrical conductivity, ρ is fluid density, μ is dynamic viscosity, c_p is specific heat at constant pressure, j is the micro rotation viscosity, κ is the vortex viscosity, k is the thermal conductivity, and N is micro rotation velocity. The boundary conditions of the problem can be expressed as follows:

$$u=0, \qquad v=0, \qquad T=T_1,$$

$$N=-s\frac{\partial u}{\partial y}=0, \qquad \text{at} \quad y=0, \qquad (11)$$

$$u=0, \qquad v=-v_w, \qquad T=T_2,$$

$$N=-s\frac{\partial u}{\partial y}=0, \qquad \text{at} \quad y=a(t). \qquad (12)$$

$N=0$ represents that the microelements, which are close to the wall, are impotent to rotate. The temperature of the fluid at distance η from the wall is defined as follows:

$$T=T_1+\sum C_m(x/a)^m\theta_m(\eta), \qquad (13)$$

along with the corresponding boundary conditions:

$$\theta_m(0)=1, \qquad \theta_m(1)=0. \qquad (14)$$

When the wall temperature is expressed as a polynomial variation (Eq. (13)), calculating a single value for the heat transfer coefficient along the hot wall is not possible. Therefore, the hot wall temperature should be considered as:

$$T_2=T_1+\sum C_m(x/a)^m\theta_m(0). \qquad (15)$$

The similarity parameters are defined as:

$$u=-\frac{v}{a^2}xF_\eta(\eta,t), \qquad v=\frac{\nu}{a}xF_\eta(\eta,t),$$

$$N=\frac{\nu}{a^3}xG(\eta,t), \qquad \eta=\frac{y}{a(t)}. \qquad (16)$$

When the above parameters are put in Eqs. (6) to (10), by using the relations of Majdalani et al. [38], these equations change as follows (Eqs. (17) to (19)):

$$\left(1+\frac{q}{A_2}\right)\left(\frac{A_2}{A_1}\right)f^{(4)}-\frac{q}{A_1}g''+3\alpha f''+\alpha\eta f'''$$

$$+(f'f''-ff''')R-\frac{A_5}{A_1}Ha^2f''=0, \qquad (17)$$

$$\left(1+\frac{q}{2A_2}\right)\left(\frac{A_2}{A_1}\right)g''+\alpha\xi\left(3g+\eta g'\right)+R\xi f'g$$

$$-R\xi fg'-\frac{q}{A_2}\left(\frac{A_2}{A_1}\right)(2g-f'')=0, \qquad (18)$$

$$\theta''=\Pr\left(\frac{A_4}{A_3}\right)(-\alpha)\left(m\theta_m+\eta\theta_m'\right)$$

$$-\Pr\left(\frac{A_4}{A_3}\right)R\left(mf'\theta_m+f\theta_m'\right), \qquad (19)$$

where $q=\kappa/\mu_f$ and $\xi=j/a^2$. $\alpha=a\dot{a}/v_f$ is the expansion ratio and it is positive when we have expansion and negative when we have contraction; also, m is the temperature power index. The other parameters are as follows:

$$A_1=\frac{\rho_{nf}}{\rho_f}, \qquad A_2=\frac{\mu_{nf}}{\mu_f}, \qquad A_3=\frac{(\rho c_p)_{nf}}{(\rho c_p)_f},$$

$$A_4=\frac{k_{nf}}{k_f}, \qquad A_5=\frac{\sigma_{nf}}{\sigma_f}, \qquad (20)$$

$$f=\frac{F}{R}, \qquad g=\frac{G}{R}, \qquad \text{Re}=\frac{v_w}{v_f},$$

$$Ha^2=\frac{\sigma_f B^2 a^2}{\mu_f}. \qquad (21)$$

It is worth mentioning that the Reynolds number is positive for suction and negative for injection. Ha is the Hartmann number.

The boundary conditions are:

$$\theta(1)=0, \quad f(1)=1,$$

$$f'(1)=0, \quad g(1)=0, \qquad (22)$$

$$\theta(0)=1, \quad f(0)=0,$$

$$f'(0)=0, \quad g(0)=0. \qquad (23)$$

In this case, the non-dimensional Nusselt number is given by:

$$\text{Nu}=-A_3\frac{\partial T}{\partial \eta}/(T_2-T_1)=-A_3\theta_m''(0). \qquad (24)$$

3. Analysis of the least square method

One of the approximation techniques for solving differential equations is the Weighted Residual Methods (WRMs). The weighted residual methods are general and powerful methods to obtain approximate solutions to Ordinary Differential Equations (ODEs) or Partial Differential Equations (PDEs). Consider the following (partial) differential equation:

$$L_m(\phi) = f \qquad \text{in} \quad \Omega, \tag{25}$$

where L_m denotes the differential operator with the highest order of derivative m in the Ω domain, ϕ is the unknown function, and f is a given function. The aim of the solution is to seek a solution for ϕ, which satisfies Eq. (25).

Assume that ϕ is approximated by a function, Φ^* (trail solution), which is a linear combination of basic functions chosen from a linearly autonomous set. That is:

$$\Phi \cong \Phi^* = \sum_{i=1}^n c_i \Phi_i. \tag{26}$$

By substituting Eq. (26) into Eq. (25), the result of the operations is not generally f. It results in the so-called residual, Rs, defined as:

$$Rs = L_m(\Phi^*) - f. \tag{27}$$

We can use some techniques to properly obtain an approximate function so as to make the residual as "small" as possible; we push the residual toward zero in an average sense by setting weighted integrals of residuals to zero. For instance, we impose:

$$\int_\Omega Rs W_i d\Omega = 0, \qquad i = 1, 2, 3, \cdots, n. \tag{28}$$

Note that in WRMs, the number of weight functions, W_i, always equals the number of unknown constants, c_i, in Φ^*. This yields n algebraic equations for the unknown constants, c_i. In the LSM method, the sum of all the squares of the residues should be minimized:

$$\zeta = \int_\Omega Rs^2 d\Omega = \sum_{i=1}^n \int_{\Omega_i} Rs_i^2 d\Omega$$

$$= \sum_{i=1}^n \int_{\Omega_i} [L_m(\Phi_i^*) - f_i] d\Omega. \tag{29}$$

In order to achieve a minimum of the functional ζ, the derivatives of ζ with respect to all the unknown parameters must be zero. That is:

$$\frac{\partial \zeta}{\partial c_i} = 2 \int_\Omega Rs \frac{\partial R}{\partial c_i} d\Omega = 0. \tag{30}$$

The weight functions are obtained in comparison with Eq. (28) (The Eq. (30) should be zero. So, the constant number of 2 cannot be considered):

$$W_i = \frac{\partial Rs}{\partial c_i}. \tag{31}$$

In order to use the least square method in this problem, the considered functions must satisfy the boundary conditions of the problem. These functions are generally considered as Eqs. (38) to (41):

$$f = y^2 + c_1(y^2 - y^3) + c_2(y^2 - y^4) + c_3(y^2 - y^5)$$
$$+ c_4(y^2 - y^6) + c_5(y^2 - y^7), \tag{32}$$

$$f' = 2y + c_1(2y - 3y^2) + c_2(2y - 4y^3)$$
$$+ c_3(2y - 5y^4) + c_4(2y - 6y^5) + c_5(2y - 7y^6), \tag{33}$$

$$g = c_6(y - y^2) + c_7(y - y^3) + c_8(y - y^4) + c_9(y - y^5), \tag{34}$$

$$q = 1 - y + c_{10}(y - y^2) + c_{11}(y - y^3)$$
$$+ c_{12}(y - y^4) + c_{13}(y - y^5). \tag{35}$$

By introducing these equations into Eqs. (17) to (19), the residual function is obtained and by substituting the residual functions into Eqs. (32) to (35), a set of equations will be obtained; by solving these algebraic equations, coefficients c_1-c_{13} will be determined.

In order to make a comparison between the numerical results and the previous literature, the results of Sheikholeslami et al. [35] have been used. They examined the flow of nanofluid in a semi-porous channel by using the least square and Galerkin methods. In Figure 3, our results and those of Sheikholeslami et al. [35] have been presented for Re = 0.5, Ha = 0.5, and $\phi = 0.05$.

4. Numerical method

In order to solve the governing equations numerically, the fourth order Runge-Kutta-Fellberg method is employed. This method is applicable to the problems with definite boundary conditions. Moreover, in this method, the equations are solved for two time steps of h and $h/2$, and the results of the larger time step are compared with the smaller ones until the problem reaches the considered accuracy. Indeed, this method is employed to solve various engineering and mathematical equations [39].

5. Results and discussion

In this study, flow field, heat transfer, and micro rotation of Al_2O_3-Cu/water micropolar hybrid nanofluid
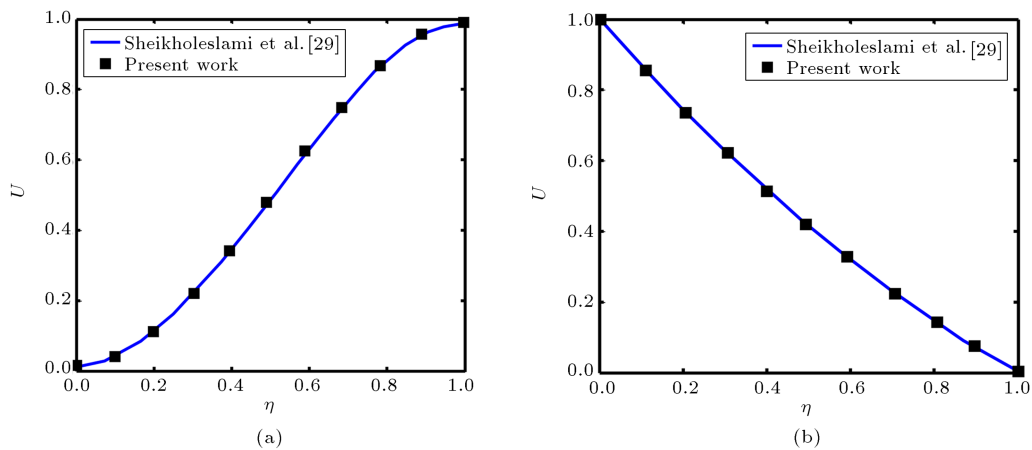
Figure 3. The comparisons of (a) the V velocity and (b) the U velocity, for Re = 0.5, Ha = 0.5, and $\phi = 0.05$.

are examined in a porous channel with expanding or contracting wall in the presence of a magnetic field. The effect of considering the micro rotation of nanoparticles is compared with when it is not taken into account. Moreover, the effects of parameters such as Re, Ha, ϕ, q, and α on the flow filed and heat transfer are investigated. The study is performed with Re = 1 to 7; Ha = 0 to 6; $\alpha = -1$, 0, and 1; $q = 0.1$, 0.3, and 0.5; $\phi = 0.00$ to 0.02; Pr = 6.2; $m = 4$; and $\xi = 1$.

In Tables 2 and 3, the components of velocity (axial velocity f and normal velocity f'), temperature (θ), and micro rotation (g), which are obtained from LSM, are compared with those of NUM method with $\phi = 0.02$, $q = 0.2$, Re = 1, and $\alpha = -1$. The relative difference between the values obtained from LSM and NUM results is negligible and ensures accuracy of the modeling results.

The plots in Figure 4 elucidate the effect of Reynolds number on velocity, temperature, and micro rotation profiles with $\phi = 0.02$, $q = 0.2$, and $\alpha = -1$.
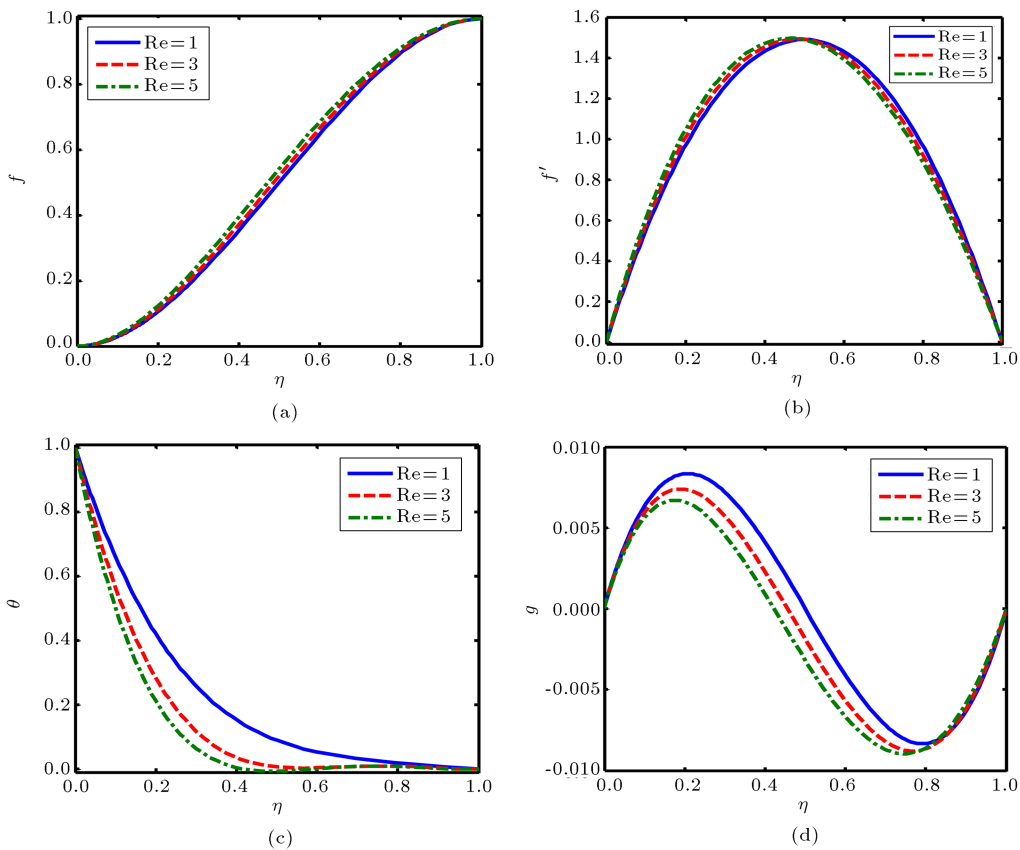
It would be obvious that with increasing Reynolds number, the axial velocity component increases and the temperature of the hybrid nanofluid decreases. The normal velocity component for $\eta < 0.5$ increases as Reynolds number increases and its behavior is reverse for $\eta > 0.5$. Also, the micro rotation parameter decreases as Reynolds number increases near the hot wall and by approaching the porous wall, the amount of micro rotation increases when Reynolds number increases. It is worth mentioning that according to the considered boundary conditions ($S = 0$), the micro rotation value near the walls becomes zero. The plot in Figure 5 represents the effect of expanding ratio (α) on velocity, temperature, and micro rotation profiles with $\phi = 0.02$, $q = 0.2$, and Re = 1. $\alpha > 0$ corresponds to expanding and $\alpha < 0$ indicates contracting. As can be seen in Figure 5, the axial velocity component is in direct relation to expanding ratio. The normal velocity component and the temperature of the hybrid nanofluid increase up to a definite η and after that, they

Table 2. Comparison of LSM and NUM results for velocity profiles with $\phi = 0.02$, $q = 0.2$, Re = 1, and $\alpha = -1$.

η	$f(\eta)$			$f'(\eta)$		
	LSM	**NUM**	**Error**	**LSM**	**NUM**	**Error**
0	0.00000000	0.00000000	0.00000000	0.00000000	0.00000000	0.00000000
0.1	0.02917309	0.02917295	0.00047989	0.54827581	0.55050308	0.40458923
0.2	0.10679572	0.10679441	0.00122664	0.96545463	0.96686954	0.14633963
0.3	0.21922307	0.21922037	0.00123162	1.25830152	1.25781497	0.03868196
0.4	0.35410971	0.35410737	0.00066081	1.43190349	1.42976114	0.14983999
0.5	0.50000000	0.50000000	0.00000000	1.48941470	1.48663604	0.18690899
0.6	0.64589029	0.64589263	0.00036229	1.43190349	1.42976114	0.14983995
0.7	0.78077693	0.78077963	0.00034581	1.25830152	1.25781497	0.03868188
0.8	0.89320428	0.89320559	0.00014666	0.96545462	0.96686954	0.14633973
0.9	0.97082691	0.97082705	0.00001442	0.54827580	0.55050308	0.40458934
1.0	1.00000000	1.00000000	0.00000000	0.00000000	0.00000000	0.00000000

Table 3. Comparison of LSM and NUM results for temperature and micro rotation profiles with $\phi = 0.02$, $q = 0.2$, Re = 1, and $\alpha = -1$.

η	$g(\eta)$			$\theta(\eta)$		
	LSM	**NUM**	**Error**	**LSM**	**NUM**	**Error**
0	0.00000000	0.00000000	0.00000000	1.00000000	1.00000000	0.00000000
0.1	0.00633552	0.00632298	0.19793166	0.66112939	0.65901257	0.32121087
0.2	0.00833333	0.00830308	0.36300015	0.42079717	0.41804123	0.65925076
0.3	0.00722040	0.00718557	0.48238325	0.25783505	0.25709804	0.28666496
0.4	0.00410151	0.00407876	0.55467377	0.15306938	0.15442755	0.87948685
0.5	0.00000000	0.00000000	0.00000000	0.09062197	0.09131136	0.75498821
0.6	-0.00410151	-0.00407876	0.55467377	0.05321083	0.05350100	0.54236369
0.7	-0.00722040	-0.00718557	0.48238325	0.03085096	0.03099348	0.45983865
0.8	-0.00833333	-0.00830308	0.36300015	0.01715511	0.01715060	0.02629646
0.9	-0.00633552	-0.00632298	0.19793166	0.00763459	0.00771571	0.24469556
1.0	0.00000000	0.00000000	0.00000000	0.00000000	0.00000000	0.00000000

Figure 4. Effects of Reynolds number on velocity, temperature, and micro rotation profiles with $\phi = 0.02$, $q = 0.2$, and $\alpha = -1$.

decrease. Figure 5(d) shows the effect of expanding ratio on micro rotation parameter. Generally, when the walls are expanded, the micro rotation parameter increases. Moreover, two critical points in the distance between two walls of channel are observed in this figure; moreover, micro rotation near the center of the channel has inflection point and its value in this point is zero.

The effect of q on velocity, temperature, and micro rotation profiles for $\phi = 0.02$, $\alpha = -1$, and Re = 1 are depicted in Figure 6. According to this figure, the impact of this parameter on the velocity and temperature components is negligible. Furthermore, with increasing q, the micro rotation parameter increases. In different values of q, the micro rotation curve still
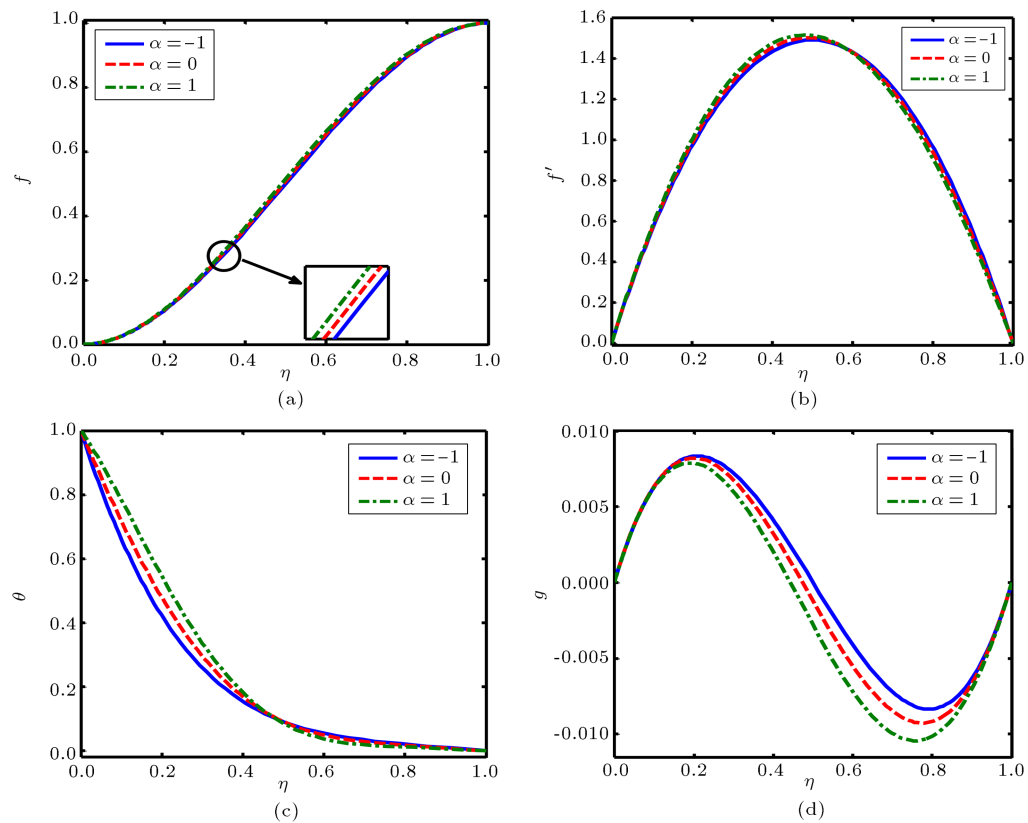
Figure 5. Effects of expanding ratio on velocity, temperature, and micro rotation profiles with $\phi = 0.02$, $q = 0.2$, and Re = 1.
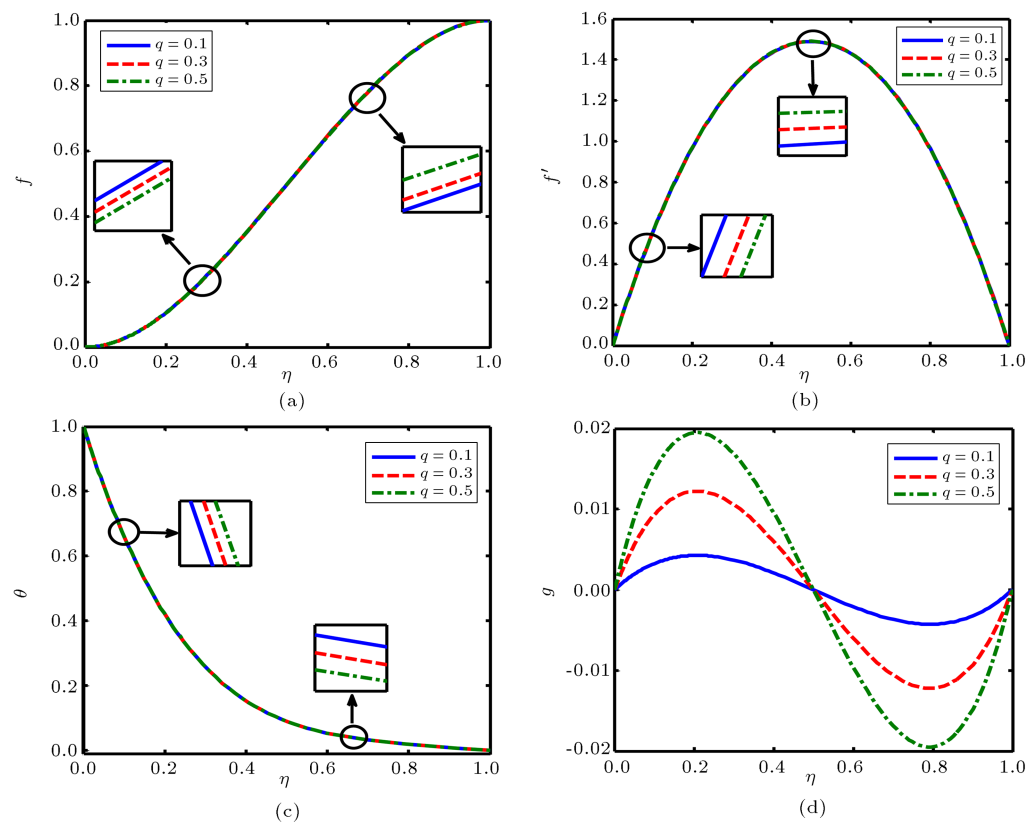

Figure 6. Effects of expanding ratio on velocity, temperature, and micro rotation profiles with $\phi = 0.02$, $\alpha = -1$, and Re = 1.
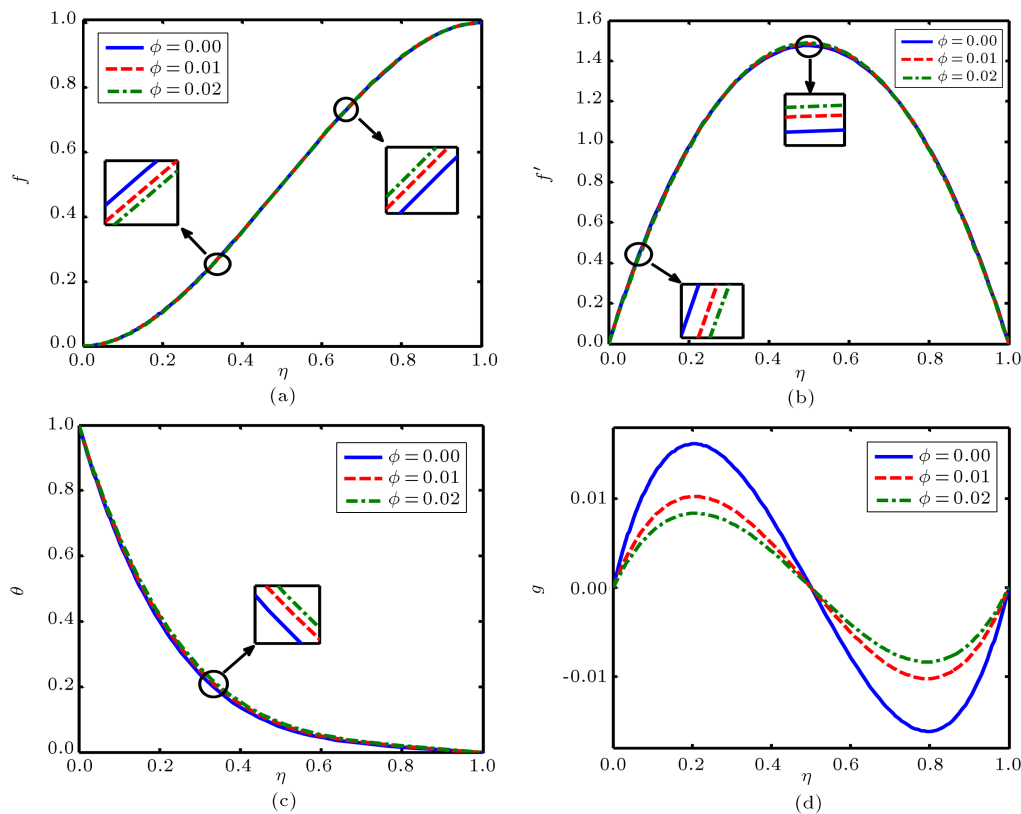
Figure 7. Effects of volume fraction of nanoparticles on velocity, temperature, and micro rotation profiles with $q = 0.2$, $\alpha = -1$, and $\mathrm{Re} = 1$.

has three points that are zero, which indicates that, in addition to the top and bottom walls which have the micro rotation, in the center of the channel, this characteristic is zero, too. Figure 7 displays the influence of nanoparticles volume fraction on velocity, temperature, and micro rotation distribution for $q = 0.2$, $\alpha = -1$, and $\mathrm{Re} = 1$. As can be concluded from this figure, the axial velocity component decreases with increasing the volume fraction of nanoparticles in lower amounts of η. The normal velocity components decrease as the volume fraction increases through the channel with the exception of the center of the channel. As expected, the temperature of micropolar hybrid nanofluid is in direct relation to volume fraction of nanoparticles. By adding more nanoparticles to the fluid, the micro rotation parameter diminishes, but the critical point and inflection points in the curve remain fixed. In order to have a better insight into the temperature power index, Figure 8 shows the variation of temperature versus η in different temperature power indices. The effect of temperature power index on temperature distribution is more perceptible in the center of the channel; as it increases, the amount of temperature decreases. Variation of Nusselt number in terms of volume fraction of nanoparticles with different Hartmann numbers is illustrated in Figure 9. As it has been proven in the literature, with increasing volume
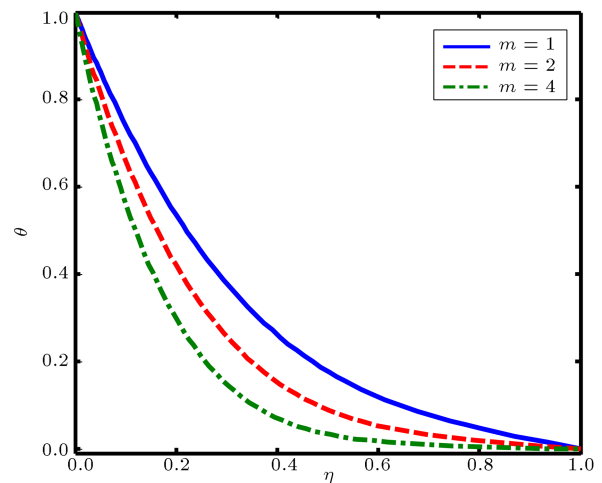

Figure 8. Effects of temperature power index on temperature distribution with $q = 0.2$, $\alpha = -1$, and $\mathrm{Re} = 1$.

fraction of nanoparticles, Nusselt number increases. Also, in order to find out the effect of magnetic field on flow field and heat transfer, the Hartmann number has been introduced. When the Hartmann number increases, Nusselt number increases and, as a result, the heat transfer increases. Therefore, in these types of problems, increasing the Hartmann number is an approach to enhance heat transfer. In Figure 10,
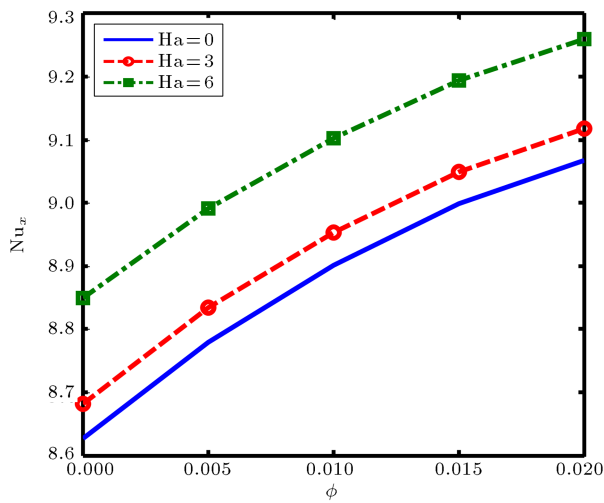
Figure 9. Variation of Nusselt number in terms of volume fraction of nanoparticles with different Hartmann numbers.

Figure 11. Comparison of using Al_2O_3 and Cu nanoparticles and hybrid of Al_2O_3-Cu nanoparticles with $\phi = 0.02$.

nanofluid than that of water-Al_2O_3 nanofluid as well as the reverse effect of the magnetic field on the heat transfer, the difference between the Nusselt numbers of the two nanofluids is reduced compared with the case that there is no magnetic field.

Comparisons of applying micropolar model of hybrid nanofluid with non-micropolar model are illustrated in Figure 12. When the micropolar theory is considered, the axial and normal velocities are less than those when the micropolar theory is not taken into account near the hot wall, but this behavior is reverse near the porous wall. In addition, the amount of temperature is high when the micropolar theory is considered. Also, the effect of Hartmann number on velocity and temperature profiles is visible in this figure. With increasing the Hartmann number, the axial velocity close to the hot wall increases and by approaching the porous wall, it decreases. In the absence of magnetic field, the normal velocity is maximum in the center of the channel. Furthermore, the magnetic field has reduction effect on temperature distribution.
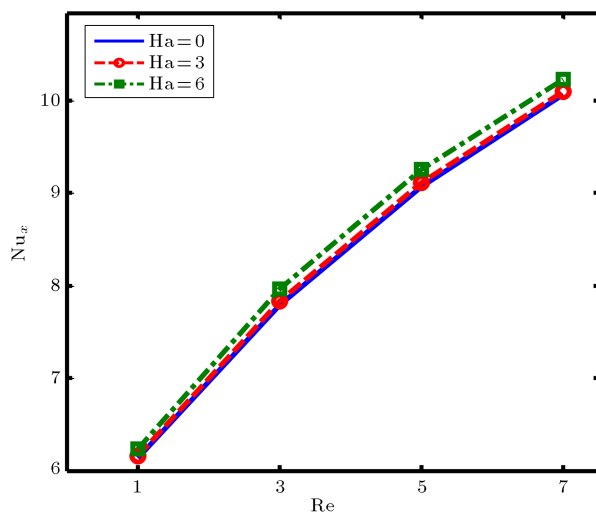

Figure 10. Variations of Nusselt number in terms of Reynolds number with different Hartmann numbers.

variation of Nusselt number with Reynolds number in different Hartmann numbers is shown. Increasing the Reynolds number leads to increase in the Nusselt number and Hartmann numbers. In order to compare the effects of using Al_2O_3 nanoparticles and hybrid of Al_2O_3-Cu nanoparticles, the proportion of the hybrid nanofluid Nusselt number to pure-fluid Nusselt number in terms of Reynolds number is indicated in Figure 11. It is obvious in this figure that the hybrid nanofluid has better thermal conductivity than common nanofluid; thus, it improves heat transfer. Also, it should be mentioned that the properties of nanofuid are determined using Maxwell model [40] and Brickman model [41]. In cases in which the magnetic field is applied, using hybrid nanofluids is preferred to using ordinary nanofluids. Moreover, it is observed that due to higher electrical conductivity of water-Cu
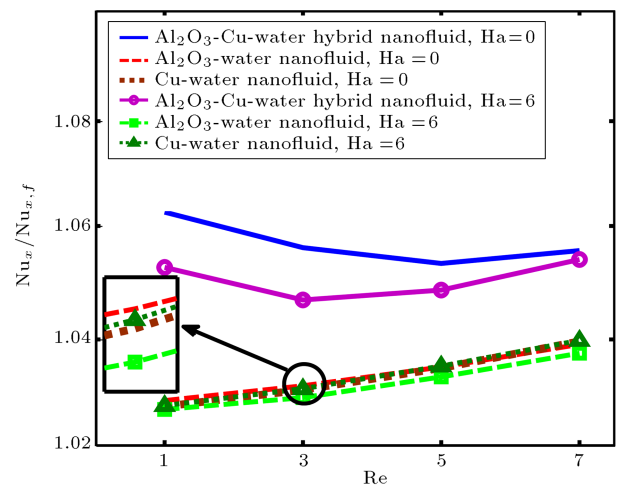
6. Conclusion

Forced convection flow and heat transfer of Al_2O_3-Cu/water micropolar hybrid nanofluid were studied in a porous channel in the presence of a magnetic field. In order to solve the governing equations, the LSM analytical method and fourth order Runge-Kutta-Fellberg numerical method were used and an excellent agreement between these two methods was observed. The impact of different parameters such as Reynolds number, Hartmann number, expanding ratio, and volume fraction of nanoparticles on velocity, temperature, and micro rotation profiles was examined. Furthermore, the effects of employing hybrid nanofluid
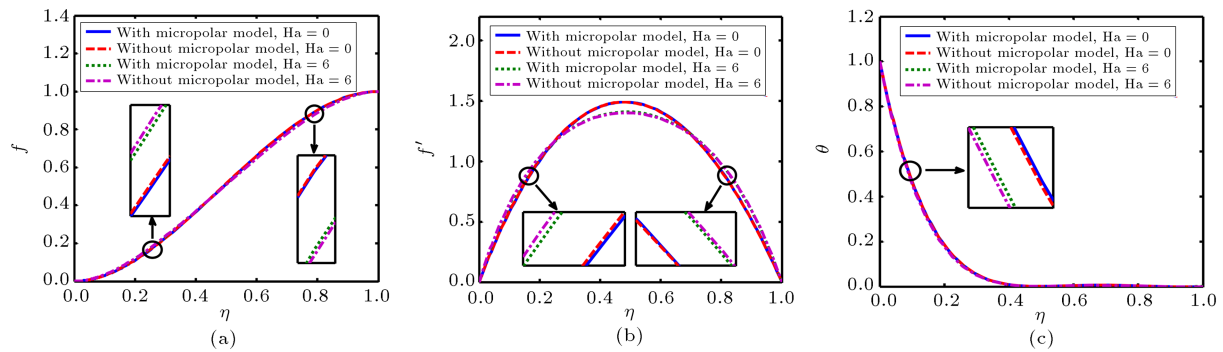
Figure 12. Comparison of applying micropolar model of hybrid nanofluid and non-micropolar model for (a) f, (b) f', and (c) θ.

and applying micropolar theory on flow field and heat transfer were investigated. According to the results:

- With increasing the Reynolds number, the temperature of hybrid nanofluid decreases;

- As the wall is expanded, the micro rotation parameter decreases;

- When the nanoparticles are added to the base fluid, the temperature of the hybrid nanofluid and Nusselt number increase significantly;

- Hartmann number is in direct relation to the Nusselt number;

- When the hybrid nanofluid is used instead of common nanofluids, the heat transfer increases considerably.

Acknowledgment

Nomenclature

f	Dimensionless stream function
g	Dimensionless micro rotation
LSM	Least Square Method
NUM	Fourth order Runge-Kutta-Fellberg numerical method
j	Micro-inertia density
N	Micro rotation/angular velocity
a	Distance between parallel walls
$a(t)$	Expand or contract function
c_p	Specific heat at constant pressure $(\mathrm{jkg^{-1}K^{-1}})$
A_{1-5}	Constant parameters in nanofluids
k	Coefficient of thermal conductivity $(\mathrm{Wm^{-1}K^{-1}})$
m	Temperature power index

Nu	Nusselt number
P	Pressure (Pa)
Pr	Prandtl number
Ha	Hartmann number
q	Micro rotation factor
Rs	Residual function
Re	Reynolds number
T	Temperature (K)
u, v	Velocity components in x and y direction
v_w	Velocity of cooling injection fluid
x	Horizontal axes coordinate
y	Vertical axes coordinate

Greek symbols

η	Similarity variable
σ	Electrical conductivity
α	Expansion ratio
ϕ	Nanoparticle volume fraction
θ	Dimensionless temperature
ρ	Density$(\mathrm{kgm^{-3}})$
μ	Dynamic viscosity
ν	Kinematic viscosity
κ	Coupling coefficient
ψ	Stream function$(\mathrm{m^2s^{-1}})$
Φ^*	Trial function

Subscripts

f	Fluid
nf	Nanofluid
s	Solid
p	Particle

References

1. Aziz, A. and Bouaziz, M.N. "A least square method for a longitudinal fin with tempreture dependent internal

heat generation and thermal conductivity", *Energy Convers. Manage.*, **52**(8-9), pp. 2876-2882 (2011).

2. Hatami, M. and Ganji, D.D. "Thermal and flow analysis of microchannel heat sink (MCHS) cooled by Cu-water nanofluid using porous media approach and least square method", *Energy Convers. Manage.*, **78**, pp. 347-358 (2014).

3. Hatami, M. and Ganji, D.D. "Natural convection of sodium alginate (SA) non-Newtonian nanofluid flow between two vertical flat plates by analytical and numerical methods", *Case Studies in Thermal Engineering*, **2**, pp. 14-22 (2014).

4. Ghasemi, S.E., Hatami, M., Mehdizadeh Ahangar, GH.R. and Ganji, D.D. "Electrohydrodynamic flow analysis in a circular cylindrical conduit using least square method", *Journal of Electrostatics*, **72**, pp. 47-52 (2014).

5. Hatami, M., Sheikholeslami, M., Hosseini, M. and Ganji, D.D. "Analytical investigation of MHD nanofluid flow in non-parallel walls", *J. Mol. Liq.*, **194**, pp. 251-259 (2014).

6. Fakour, M., Ganji, D.D. and Abbasi, M. "Scrutiny of underdeveloped nanofluid MHD flow and heat conduction in a channel with porous walls", *Case Studies in Thermal Engineering*, **4**, pp. 202-214 (2014).

7. Fakour, M., Vahabzadeh, A. and Ganji, D.D. "Study of heat transfer and flow of nanofluid in permeable channel in the presence of magnetic field", *Propulsion and Power Research*, **4**, pp. 50-62 (2015).

8. Darzi, M., Vatani, M., Ghasemi, S.E. and Ganji D.D. "Effect of thermal radiation on velocity and temperature fields of a thin liquid film over a stretching sheet in a porous medium", *Phys. J. Plus*, **130**(5), pp. 89-100 (2015).

9. Abbaszadeh, M., Ababaei, A., Abbasian Arani, A.A. and Abbasi Sharifabadi, A. "MHD forced convection and entropy generation of CuO-water nanofluid in a microchannel considering slip velocity and temperature jump", *J. Braz. Soc. Mech. Sci. Eng.*, **36**(9), pp. 775-790 (2016).

10. Sheikhzadeh, G., Aghaei, A., Ehteram, H. and Abbaszadeh, M. "Analytical study of parameters affecting entropy generation of nanofluid turbulent flow in channel and micro-channel", *Thermal Sci.*, **20**(6), pp. 2037-2050 (2016).

11. Sheikhzadeh, G., Ghasemi, H. and Abbaszadeh, M. "Investigation of natural convection boundary layer heat and mass transfer of MHD water-AL$_2$O$_3$ nanofluid in a porous medium", *International Journal of Nano Studies & Technology (IJNST)*, **5**, pp. 110-122 (2016).

12. Rahmati, A., Roknabadi, A.R. and Abbaszadeh, M. "Numerical simulation of mixed convection heat transfer of nanofluid in a double lid-driven cavity using lattice Boltzmann method", *Alexandria Engineering Journal*, **55**(4), pp. 3101-3114 (2016).

13. Wang, X., Xu, X. and Choi, S. "Thermal conductivity of nanoparticle-fluid mixture", *J. Thermophys Heat Transfer.*, **13**, pp. 474-480 (1999).

14. Selvakumar, P. and Suresh, S. "Use of Al$_2$O$_3$-Cu/water hybrid nanofluid in an electronic heat sink, components", *Packaging and Manufacturing Technology*, **2**, pp. 1600-1607 (2012).

15. Madhesh, D., Parameshwaran, R. and Kalaiselvam, S. "Experimental investigation on convective heat transfer and rheological characteristics of Cu-TiO$_2$ hybrid nanofluids", *Exp. Therm Fluid Sci.*, **52**, pp. 104-115 (2014).

16. Esfe, M.H., Abbasian Arani, A.A., Rezaie, M., Yan, W. and Karimipour, A. "Experimental determination of thermal conductivity and dynamic viscosity of Ag-MgO/water hybrid nanofluid", *International Communications in Heat and Mass Transfer*, **66**, pp. 189-195 (2015).

17. Ho, C.J., Huang, J.B., Tsai, P.S. and Yang, Y.M. "Preparation and properties of hybrid water-based suspension of Al$_2$O$_3$ nanoparticles and MEPCM particles as functional forced convection fluid", *International Communications in Heat and Mass Transfer*, **37**, pp. 490-494 (2010).

18. Suresh, S., Venkitaraj, K.P., Selvakumar, P. and Chandrasekar, M. "Synthesis of Al$_2$O$_3$-Cu/water hybrid nanofluids using two step method and its thermo physical properties", *Colloids and Surfaces A: Physicochemical and Engineering Aspects*, **388**, pp. 41-48 (2011).

19. Suresh, S., Venkitaraj, K.P., Selvakumar, P. and Chandrasekar, M. "Effect of Al$_2$O$_3$-Cu/water hybrid nanofluid in heat transfer", *Exp. Therm Fluid Sci.*, **38**, pp. 54-60 (2012).

20. Abbasia, S.M., Rashidib, A., Nematia, A. and Arzania, K. "The effect of functionalisation method on the stability and the thermal conductivity of nanofluid hybrids of carbon nanotubes/gamma alumina", *Ceram. Int.*, **39**, pp. 3885-3891 (2013).

21. Balla, H., Abdullah, S., MohdFaizal, W., Zulkifli, R. and Sopian, K. "Numerical study of the enhancement of heat transfer for hybrid CuO-Cu nanofluids flowing in a circular pipe", *Journal of Oleo Science*, **62**, pp. 533-539 (2013).

22. Takabi, B. and Salehi, S. "Augmentation of the heat transfer performance of a sinusoidal corrugated enclosure by employing hybrid nanofluid", *Advances in Mechanical Engineering*, **6**, pp. 1459-1470 (2014).

23. Moghadassi, A., Ghomi, E. and Parvazian, F. "A numerical study of water based Al$_2$O$_3$ and Al$_2$O$_3$-Cu hybrid nanofluid effect on forced convective heat transfer", *Int. J. Therm. Sci.*, **92**, pp. 50-57 (2015).

24. Mollamahdi, M., Abbaszadeh, M. and Sheikhzadeh, G.A. "Flow field and heat transfer in a channel with a permeable wall filled with Al2O$_3$-Cu/water micropolar hybrid nanofluid, effects of chemical reaction and magnetic field", *Journal of Heat and Mass Transfer Research*, **3**(2), pp. 101-114 (2016).

25. Eringen, A.C., *Journal of Mathematical Analysis and Applications*, **16**, pp. 1-18 (1966).

26. Nadeem, S., Rehman, A., Vajravelu, K., Lee, J. and Lee, C. "Axisymmetric stagnation flow of a micropolar nanofluid in a moving cylinder", Hindawi Publishing Corporation, Mathematical Problems in Engineering (2012).

27. Si, X., Zheng, L., Lin, P., Zhang, X. and Zhang, Y. "Flow and heat transfer of a micropolar fluid in a porous channel with expanding or contracting walls", *Int. J. Heat. Mass. Tran.*, **67**, pp. 885-895 (2013).

28. Bourantas, G.C. and Loukopoulos, V.C. "Modeling the natural convective flow of micropolar nanofluids", *Int. J. Heat. Mass. Tran.*, **68**, pp. 35-41(2014).

29. Sheikholeslami, M., Ashorynejad, H.R., Ganji, D.D. and Rashidi, M.M. "Heat and mass transfer of a micropolar fluid in a porous channel", *Communications in Numerical Analysis*, pp. 1-20 (2014).

30. Cao, L., Si, X. and Zheng, L. "The flow of a micropolar fluid through a porous expanding channel: A Lie group analysis", *Applied Mathematics and Computation*, **270**, pp. 242-250 (2015).

31. Das, S.K., Choi, S.U.S., Yu, W. and Predeep, T., *Nanofluids Science and Technology*, John Wiley & Sons (2008).

32. Nimmagadda, R. and Venkatasubbaiah, K. "Conjugate heat transfer analysis of micro-channel using novel hybrid nanofluids", *European Journal of Mechanics-B/Fluids*, **52**, pp. 19-27 (2015).

33. Xuan, Y. and Roetzel, W. "Conceptions for heat transfer correlations of nanofluids", *Int. J Heat. Mass. Tran.*, **43**, pp. 3701-3707 (2000).

34. Aghaei, A., Khorasanizadeh, H., Sheikhzadeh, G. and Abbaszadeh, M. "Numerical study of magnetic field on mixed convection and entropy generation of nanofluid in a trapezoidal enclosure", *J. Magn. Magn. Mater.*, **403**, pp. 133-145 (2016).

35. Sheikholeslami, M., Hatami, M. and Ganji, D.D. "Analytical investigation of MHD nanofluid flow in a semi-porous channel", *Powder Technol.*, **246**, pp. 327-336 (2013).

36. Zhang, C., Zheng, L., Zhang, X. and Chen, G. "MHD flow and radiation heat transfer of nanofluids in porous media with variable surface heat flux and chemical reaction", *Applied Mathematical Modeling*, **39**(1), pp. 165-181 (2015).

37. Sheikholeslami, M., Hatami, M. and Ganji, D.D. "Micropolar fluid flow and heat transfer in a permeable channel using analytical method", *J. Mol. Liq.*, **194**, pp. 30-36 (2014).

38. Majdalani, J., Zhou, Zamm. C. and Angew, Z., *Math. Mech.*, **83**, pp. 181-196 (2003).

39. Aziz, A., *Heat Conduction with Maple*, Philadelphia (PA): RT Edwards (2006).

40. Maxwell, J.C., *A Treatise on Electricity and Magnetism* (1881).

41. Brinkman, H.C. "The viscosity of concentrated suspensions and solutions", *The Journal of Chemical al Physic*, **20**, p. 571 (1952).

42. Arefmanesh, A. and Mahmoodi, M. "Effects of uncertainties of viscosity models for Al_2O_3-water nanofluid on mixed convection numerical simulations", *Int. J. Therm. Sci.*, **50**, pp. 1706-1719 (2011).

Biographies

Mahdi Mollamahdi received his BS degree in Mechanical Engineering from the University of Kashan, Kashan, Iran. He also received his MS degree in Mechanical Engineering with specialty in Energy Conversion from the University of Kashan. His major interests are combustion and mathematical modeling of natural phenomena.

Mahmooud Abbaszadeh received his BS degree in Mechanical Engineering from the University of Kashan, Kashan, Iran. He also received his MS degree in Mechanical Engineering with specialty in Energy Conversion from the University of Kashan. His major interests are CFD and mathematical modeling of natural phenomena.

Ghanbar Ali Sheikhzadeh received a BS degree in Mechanical Engineering from the University of Tehran, Tehran, Iran; and MS and PhD degrees in Energy Conversion from Shahid Bahonar University of Kerman. His specific research interest is CFD. He has one book and numerous professional journal articles. He is currently Professor in the Faculty of Engineering at University of Kashan, Kashan, Iran.